

Femtosecond active plasmonics: ultrafast control of surface plasmon propagation

Z L Sámson, K F MacDonald and N I Zheludev¹

Optoelectronics Research Centre, University of Southampton, Highfield, Southampton, Hampshire, SO17 1BJ, UK

E-mail: zls@orc.soton.ac.uk

Received 14 May 2009, accepted for publication 7 July 2009

Published 17 September 2009

Online at stacks.iop.org/JOptA/11/114031

Abstract

Excitation of an aluminium/dielectric plasmonic waveguide with 200 fs optical pulses leads to the transient modulation of surface plasmon-polariton signals propagating in the waveguide. We show that by tuning the excitation wavelength to aluminium's interband absorption peak at ~ 1.5 eV, a modulation depth of more than 35% can be achieved at an excitation fluence of 13 mJ cm^{-2} . 'Fast' (femtosecond) and 'slow' (picosecond) modulation response components are observed.

Keywords: surface plasmon-polaritons, active plasmonics, nonlinear optics

(Some figures in this article are in colour only in the electronic version)

Plasmonics is currently one of the most fascinating and fast-moving fields of photonics [1–3]. The ever-improving capabilities and wider availability of nanofabrication systems, sample analysis instrumentation and computational simulation tools have made fundamental studies of nanoscale light–matter interactions possible and this has opened up a wide range of potential applications for localized surface plasmons (SPs) and propagating surface plasmon-polaritons (SPPs) alike in fields ranging from solar power generation and catalysis to super-resolution imaging and single-molecule chemical/biological sensing. Some of the most significant opportunities lie in data transport and processing, where plasmonic technologies offer to combine the small size of today's electronic systems, in which performance is becoming limited by intra-chip data transfer times, with the speed and bandwidth of photonic systems [4, 5].

With such applications in mind, all sorts of SPP waveguide configurations have been studied [3, 6, 7], and a range of structures for the passive manipulation of SPP signals have been proposed [3, 8, 9]. In recent years attention has also turned to the kind of 'active' and nonlinear components that will be required to switch and modulate SPP signals in practical devices. The term 'active plasmonics' was coined in a 2004 paper describing the concept of using an optically activated phase-change in an SPP waveguide to

control signal propagation [10]. Since that time, a range of material systems has been investigated for plasmonic switching applications [11–13]. Most recently, the performance limits for active plasmonics have been extended into the femtojoule switching energy and terahertz operating frequency domains with the demonstrations, respectively, of a compact field-effect plasmonic modulator [14] and the direct optical modulation of SPP propagation on the femtosecond timescale [15].

Here, we report on the spectral dispersion of the ultrafast optical modulation effect for an aluminium/silica SPP waveguide [15] in the vicinity of aluminium's near-infrared interband absorption peak [16]. 'Fast' (femtosecond light–SPP coherent nonlinear interaction) and 'slow' (picosecond 'Fermi smearing'/thermal) response components were reported in [15]. Both are found here to increase in magnitude with wavelength towards the absorption peak at ~ 810 nm, providing more than 35% modulation of plasmon wave intensity, though the slow (picosecond) component grows more rapidly to become the dominant component at wavelengths longer than ~ 790 nm.

Details of sample structure and the optical pump/SPP probe experimental configuration employed in this study can be found in [15]. To summarize, experiments were performed at 765, 780, 795 and 810 nm using the beam from a Ti:sapphire laser generating ~ 200 fs pulses at 250 kHz, which was split into pump and probe components mechanically chopped at different frequencies (ν_{pump} and ν_{probe}). A plasmonic probe

¹ <http://www.nanophotonics.org.uk/niz/>.

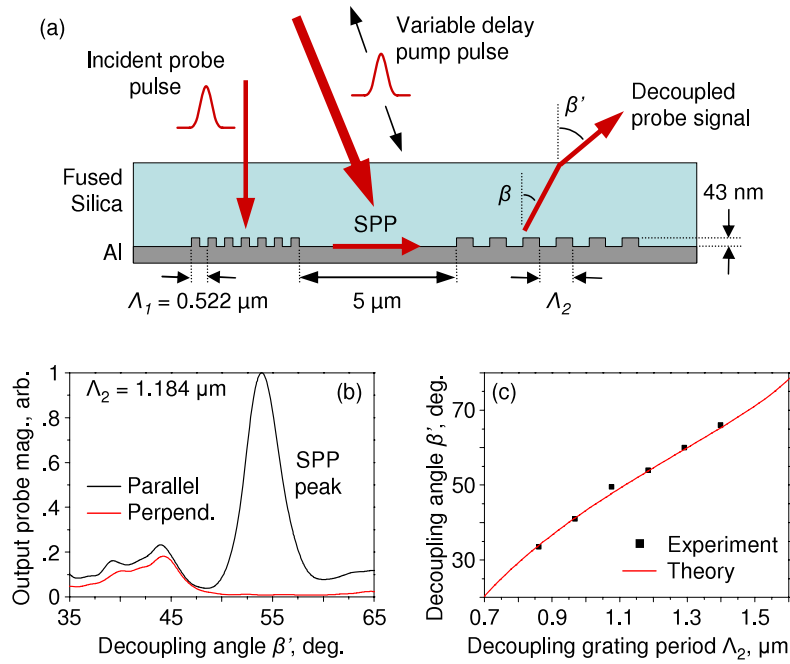


Figure 1. (a) Schematic sample geometry and pump-probe beam configuration: gratings couple/decouple probe pulses to/from an SPP wave on an Al/silica interface. Their propagation is controlled by pump pulses incident on the unstructured section of waveguide between the gratings. (b) Decoupled probe signal magnitude (in the absence of pump excitation) as a function of measured decoupling angle for an output grating period $\Lambda_2 = 1.184 \mu\text{m}$, for incident polarizations parallel (black) and perpendicular (red) to the grating vectors. (c) Measured decoupling angle as a function of grating period (black points) overlaid with a theoretical dependence (red line) derived from the grating decoupling equation (taking into account refraction at the silica/air interface).

signal was generated on an Al/silica interface by grating coupling from the probe light beam, which was focused by a $10\times$ microscope objective onto the sample at normal incidence (to a $17 \mu\text{m}$ diameter spot with fluence of 0.9 mJ cm^{-2}). This signal was detected in the optical far field after decoupling at an oblique angle by a second grating separated from the first by $5 \mu\text{m}$ of unstructured metal/dielectric interface (see figure 1(a)). The pump beam was focused at an oblique angle to a spot with a diameter of $34 \mu\text{m}$ centred on the unstructured region between the gratings. An optical delay line in the pump path was used to vary the relative arrival times of pump and probe pulses at the sample and the transient effect of pump excitation on probe SPP propagation was monitored by recording the magnitude of the decoupled probe signal at the chopping sum frequency ($\nu_{\text{pump}} + \nu_{\text{probe}}$, with a lock-in amplifier) as a function of pump-probe delay. Experiments were performed for linear pump polarizations both parallel and perpendicular to the direction of SPP propagation between the gratings.

In preliminary measurements performed at each wavelength, the plasmonic (as opposed to scattered or diffracted) nature of the probe signal was verified by recording the output signal magnitude at ν_{probe} , in the absence of pump excitation, as a function of decoupling angle for polarizations of the incident probe beam parallel and perpendicular to the grating vectors. Only the parallel polarization can be coupled/decoupled to/from an SPP wave by the gratings, and indeed it is only in the parallel case that optical output signals are observed at decoupling angles β given (after taking account of refraction at

the silica/air interface) by the conservation of momentum condition $k_{\text{SPP}} - k_G = k_d \sin \beta$, where k_{SPP} is the SPP wavevector, $k_G = 2\pi/\Lambda$ is the grating vector for a period Λ and k_d is the wavevector of light in the dielectric (see figures 1(b) and (c)). It should be noted here that the group velocity dispersion for near-infrared SPPs on an Al/silica interface is close to zero and therefore that pulse broadening during propagation between the gratings is negligible.

Time-resolved sum-frequency measurements of pump-induced probe SPP modulation reveal fast and slow response components for all wavelengths used in the present study: representative sets of data for the two orthogonal pump polarization directions at 810 nm are shown in figures 2(a) and (b). As in the original study [15] performed at 780 nm, the fast component reproduces the optical cross-correlation function of the pump and probe pulses around the zero-delay position, indicating response and relaxation times shorter than the 200 fs pulse duration, and is *only* seen when the pump polarization has a component parallel to the direction of SPP propagation (i.e. the direction of electron oscillations in the SPP wave) (figure 2(a)). The slow component, which is present regardless of pump polarization (figure 2(b)), grows during the first one to two picoseconds after excitation then recovers with an exponential decay time of ~ 60 ps.

The wavelength range covered by this study (limited by the tuning range of the femtosecond laser source) lies immediately to the higher photon-energy side of an interband absorption peak in aluminium centred at $\sim 1.5 \text{ eV}$ (see figure 3). The peak magnitude of the fast response component increases sublinearly with pump fluence as shown

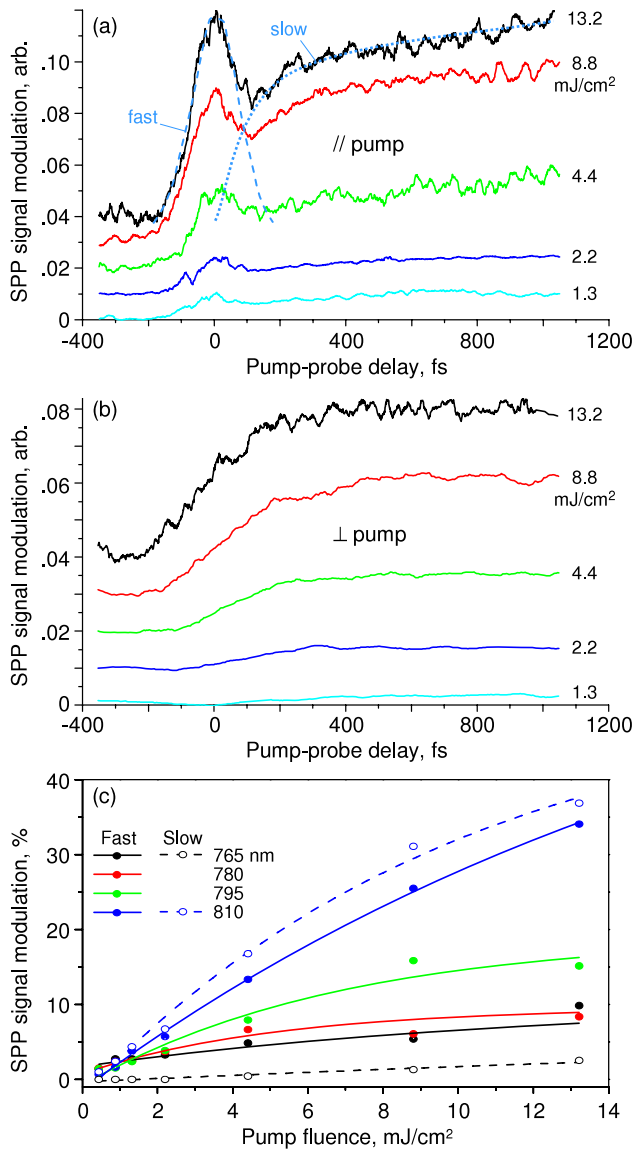


Figure 2. ((a), (b)) Transient pump-induced modulation of the decoupled SPP probe signal at 810 nm as a function of pump-probe delay for pump polarization directions parallel (a) and perpendicular (b) to the probe SPP propagation direction, for a range of pump fluences (as labelled). Traces in (a) and (b) are vertically offset by 0.01 units for clarity. (c) Peak magnitudes of the fast (closed symbols, solid lines) and slow (open symbols, dashed lines) response components as functions of pump fluence for the parallel pump polarization at a selection of wavelengths (as labelled) close to aluminium’s near-infrared interband transition. For clarity, each trace in (a) and (b) is offset from the previous trace by 0.01 units.

in figure 2(c), and quite substantially with wavelength (i.e. with proximity to the interband absorption peak) from <10% at a fluence of 13.2 mJ cm⁻² for 765 and 780 nm to >30% at the same fluence for 810 nm. The peak magnitude of the slow component also follows these trends, but its rate of increase with wavelength is even more dramatic: at 765 nm, with a pump fluence of 13.2 mJ cm⁻², it has a magnitude of less than 3% (i.e. less than one third of the corresponding fast component) but at 810 nm it exceeds the corresponding fast response peak and reaches ~35%.

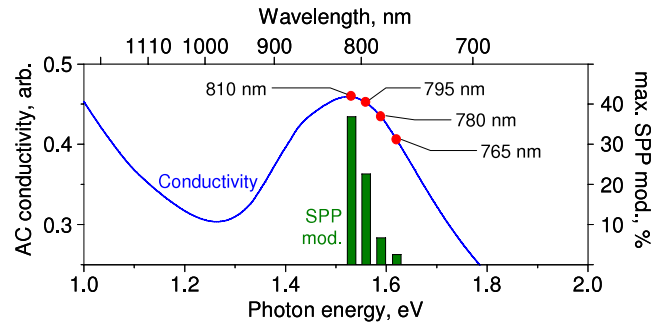


Figure 3. Optical conductivity of aluminium (after [16]), showing a peak at ~1.5 eV related to interband absorption. The red dots indicate the wavelengths used in the present study. The vertical bars show the corresponding peak magnitude of the slow SPP modulation component at maximum pump fluence (13.2 mJ cm⁻²).

These findings are consistent with the microscopic interpretation reported in [15], based on the mechanisms responsible for previously observed femtosecond-to-picosecond light-induced changes in the reflectivity of aluminium [17, 18], whereby an increase in reflectivity induced by ultrafast optical excitation coincides with lower losses for plasmon propagation manifested as an increase in the measured plasmon signal output. The fast component of the response (the zero-delay spike) results from the combination of a coherent non-linearity (related to the non-parabolicity of the electron dispersion) and coupling of wavelength degenerate pump light into the probe SPP via a transient grating created by the optical pump beam and probe SPP wave. The disappearance of the response for perpendicular polarizations is characteristic of this type of nonlinearity. The slow component results from the pump-induced excitation of numerous electrons to states above the Fermi level through an interband transition and their subsequent thermalization with the lattice—a transient response known as ‘Fermi smearing’ [19]. The initial response profile is related to a complex dynamic balance between Fermi smearing and thermal/elastic effects while the relaxation time of the slow response is related to the time needed for heat to leave the metal’s skin layer and for the lattice deformation to recover. In aluminium the free-electron absorption spectrum is strongly modified by interband transitions, primarily between parallel bands $\Sigma_3 - \Sigma_1$ in the vicinity of the $\Sigma[110]$ axis, near the K point [16], giving an optical conductivity peak at approximately 1.5 eV (see figure 3). The experiments reported here illustrate that the increasing strength of interaction between optical pump and SPP probe pulses with proximity to the absorption resonance is linked to the increasing interband absorption cross-section. Both the fast and slow response components are affected by transient changes in the density of free electrons which, for a given pump fluence, increase in magnitude with proximity to the absorption peak.

In summary, the spectral dependence of ultrafast optically induced surface plasmon-polariton modulation in an aluminium/silica waveguide has been investigated in the vicinity of the metal’s near-infrared interband absorption peak. The response comprises an ultrafast (femtosecond), polarization-dependent coherent component and a slower (picosecond) component. Both increase substantially with

increasing wavelength towards the absorption peak, but the slow component grows more rapidly and ultimately comes to dominate the response characteristic. Thus, for plasmonic signal modulation applications there is a trade-off to be made between modulation depth and operating frequency: at shorter wavelengths (e.g. 765 nm) the peak modulation depth is small (<10% even at high pump fluences), but with a fast response component around three times larger than the slow component one could operate at terahertz frequencies and beyond (limited only by electron momentum relaxation times); in contrast, at 810 nm one can achieve a modulation depth in excess of 35% but at a frequency limited (by the exponential decay dynamics of the slow component) to the few-gigahertz range. It should be noted that the depth of plasmonic signal modulation in either case may be increased using interferometric waveguide configurations.

Acknowledgments

The authors would like to acknowledge the technical assistance of D P Banks, and the financial support of the Engineering and Physical Sciences Research Council (UK).

References

- [1] Polman A 2008 *Science* **322** 868–9
- [2] Maier S A 2007 *Plasmonics—Fundamentals and Applications* (New York: Springer)
- [3] Bozhevolnyi S I (ed) 2009 *Plasmonic Nanoguides and Circuits* (Singapore: World Scientific)
- [4] Ozbay E 2006 *Science* **311** 189–93
- [5] Zia R, Schuller J A, Chandran A and Brongersma M L 2006 *Mater. Today* **9** 20–7
- [6] Dionne J A, Lezec H J and Atwater H A 2006 *Nano Lett.* **6** 1928–32
- [7] Oulton R F, Sorger V J, Genov D A, Pile D F P and Zhang X 2008 *Nat. Photon.* **2** 496–500
- [8] Ditlbacher H, Krenn J R, Schider G, Leitner A and Aussenegg F R 2002 *Appl. Phys. Lett.* **81** 1762–4
- [9] Stockman M I 2006 *Nano Lett.* **6** 2604–8
- [10] Krasavin A V and Zheludev N I 2004 *Appl. Phys. Lett.* **84** 1416–8
- [11] Nikolajsen T, Leosson K and Bozhevolnyi S I 2004 *Appl. Phys. Lett.* **85** 5833–5
- [12] Pacifici D, Lezec H J and Atwater H A 2007 *Nat. Photon.* **1** 402–6
- [13] Pala R A, Shimizu K T, Melosh N A and Brongersma M L 2008 *Nano Lett.* **8** 1506–10
- [14] Dionne J A, Diest K, Sweatlock L A and Atwater H A 2009 *Nano Lett.* **9** 897–902
- [15] MacDonald K F, Sámson Z L, Stockman M I and Zheludev N I 2009 Ultrafast active plasmonics *Nat. Photon.* **3** 55–8
- [16] Ashcroft N W and Sturm K 1971 *Phys. Rev. B* **3** 1898–910
- [17] Wilks R and Hicken R J 2004 *J. Phys.: Condens. Matter.* **16** 4607–17
- [18] Guo C, Rodriguez G, Lobad A and Taylor A J 2000 *Phys. Rev. Lett.* **84** 4493–6
- [19] Eesley G L 1986 *Phys. Rev. B* **33** 2144–51